# Production of $WS_2$ Nanotubes

Yan Qiu Zhu, Wen Kuang Hsu, Nicole Grobert, Bao He Chang, Mauricio Terrones, Humberto Terrones, Harold W. Kroto, and David R. M. Walton*

*School of Chemistry, Physics and Environmental Science, University of Sussex, Brighton, BN1 9QJ, United Kingdom*

Bing Qing Wei

*Max-Planck-Institut fur Metallforschung, Seestrasse 92, D-70174 Stuttgart, Germany, and Department of Mechanical Engineering, Tsinghua University, Beijing 100084, P. R. China*

*Received December 8, 1999*
*Revised Manuscript Received March 24, 2000*

All-carbon nanotubes[1] were discovered in 1991 and have attracted much attention because of their superior mechanical properties[2] and unique electronic behavior.[3] For an example, they have been used as microscope probes,[4] as field emission sources[5] and as reinforcements for composites.[6] Various approaches to the large-scale production of high-quality aligned carbon nanotubes have been explored, notably laser ablation,[7] arc-discharge,[8] chemical vapor deposition,[9] electrochemical growth,[10] and even solid-phase decomposition.[11] These methods in turn have provided routes to other nanomaterials, such as heteronanotubes, e.g. BN,[12] $B_xC_yN_z$,[13] and $NiCl_2$.[14] Other ceramic nanotubes have been prepared recently by various approaches: e.g. silica nanotubes by an anodic alumina template method,[15] titania nanotubes by chemical processing[16] and vanadium oxide nanotubes by a sol−gel reaction following hydrothermal treatment.[17,18] A particularly significant breakthrough was made by Tenne and co-workers[19−21] who succeeded in constructing related $MX_2$ cages (M = Mo or W; X = S, Se, Te). This work has opened up an exciting new area of research into sheet materials which, unlike single-layer graphite and double-layer B−C−N, are multiple-layer structures. These $MX_2$ species, termed inorganic fullerenes (IF),[22] are akin to carbon nanotubes in that they exhibit analogous mechanical and electronic properties. They are used as solid lubricants[23] and may be employed as nanoscale electronic devices.[24] The methods developed by Tenne et al.,[19−21] starting from commercially available $WO_3$ or $MoO_3$, result in short tubes (∼10 nm to 5 $\mu$m length) mixed with polyhedral particles. Recently, a significant breakthrough in large (micro) IF tube synthesis was reported independently by Remskar[25] and Rothschild.[26] Thus, the technology for creating IF nanostructures continues to improve. In 1996, it was estimated that 3−4 years would be required to convert one $MoS_2$ crystal into an IF nanoparticle by electron beam irradiation.[27] In practice, such nanostructures can be produced by a sonoelectrochemical procedure at room temperature with a few hours.[28] The key challenge is to devise production methods, which result in longer nanotubes accompanied by a reduction in the percentage of nanoparticles formed.

In a previous paper,[29] we described the generation of treelike microstructures consisting of large $WO_x$ nanorods ($x$ = 2−3; ∼100 $\mu$m length and 10−100 nm diameter), by heating a $SiO_2$ plate placed on a W foil in an atmosphere of Ar (100 Torr). We have now extended the investigation to creating $WS_2$ nanotubes by employing Ar (100 Torr) and $H_2S$ (100 Torr). These in-situ grown nanotubes are quite long (∼5−30 $\mu$m), are of uniform diameter (∼20−100 nm), and are obtained in quantity (∼0.5 g per run). Previous methods[30−32] used a mixture of $H_2$, $N_2$, and $H_2S$ to convert $WO_3$, via $W_{18}O_{49}$ into $WS_2$. The advantage of our new method is that control of parameters is easier in the absence of $H_2$.

(1) Iijima, S. *Nature* **1991**, *56*, 354.
(2) Sawada, S.; Hamada, N. *Solid State Commun.* **1992**, *83*, 917.
(3) Mintmire, T. W.; Dunlap, B. I.; White, C. T. *Phy. Rev. Lett.* **1992**, *68*, 631.
(4) Dai, H.; Halner, J.; Reizler, A. G.; Colbert, D. T.; Smalley, R. E. *Nature* **1996**, *384*, 147.
(5) Saito, Y.; Hamahuchi, K.; Hata, K.; Uchita, K.; Tasaka, Y.; Ikazaki, Y.; Yamura, M.; Kasuya, A.; Nishina, Y. *Nature* **1997**, *389*, 554.
(6) Kuzumaki, T.; Miyazawa, K.; Ichinose, H.; Ito, K. *J. Mater. Res.* **1998**, *13*, 2445.
(7) Guo, T.; Nikolaev, P.; Rinzler, A. G.; Tomanek, D.; Colbert, D. T.; Smalley, R. E. *J. Phy. Chem.* **1995**, *99*, 10694.
(8) Ebbesen, T. W. *Annu. Rev. Mater. Sci.* **1994**, *24*, 235.
(9) Endo, M.; Takeuchi, M.; Hare, J. P.; Terrones, H.; Kroto, H. W.; Walton, D. R. M. *Chem. Phy. Lett.* **1996**, *261*, 161.
(10) Hsu, W. K.; Hare, J. P.; Terrones, M.; Harris, P. J. F.; Kroto, H. W.; Walton, D. R. M. *Nature* **1995**, *377*, 687.
(11) Hsu, W. K.; Zhu, Y. Q.; Trasobares, S.; Terrones, H.; Terrones, M.; Grobert, N.; Takikawa, H.; Hare, J. P.; Kroto, H. W.; Walton, D. R. M. *Appl. Phys. A* **1999**, *68*, 493.
(12) Chopra, N. G.; Luyken, R. J.; Cherrey, K.; Crespi, V. H.; Cohen, M, L.; Louie, S. G.; Zettl, A. *Science* **1995**, *269*, 966.
(13) Stephan, O.; Ajayan, P. M.; Colliex, C.; Redlich, P.; Lambert, J. M.; Bernier, P.; Lefin, P. *Science* **1994**, *266*, 1683.
(14) Hachohen, Y. R.; Grunbaum, E. Tenne, R.; Sloan, J.; Hutchison, J. L. *Nature* **1998**, *395*, 336.
(15) Zhang, M.; Bando, Y.; Wada, K. *J. Mater. Res.* **2000**, *15*, 387.
(16) Kasuga, T.; Hiramatsu, M.; Hoson, A.; Sekino, T.; Niihara, K. *Adv. Mater.* **1999**, *11*, 1307.
(17) Muhr, H. J.; Krumeich, F.; Schonholzer, U. P.; Bieri, F.; Niederberger, M.; Gauckler, L. J.; Nesper, R. *Adv. Mater.* **2000**, *12*, 231.
(18) Krumeich, F.; Muhr, H. J.; Niederberger, M.; Bieri, F.; Schnyder, B.; Nesper, R. *J. Am. Chem. Sci.* **1999**, *12*, 8324.
(19) Tenne, R.; Margulis, L.; Genut, M.; Hodes, G. *Nature* **1992**, *360*, 444.
(20) Margulis, L.; Salltra, G.; Tenne, R.; Talianker, M. *Nature* **1993**, *365*, 144.
(21) Tsirlina, T.; Feldman, Y.; Homyonfer, M.; Sloan, j.; Hutchison, J. l.; Tenne, R. *Fullerene Sci. Technol.* **1998**, *6*, 157.
(22) Tremel, W. *Angew. Chem., Int. Ed. Engl.* **1999**, *38*, 2175.
(23) Rapoport, L.; Feldman, Y.; Homyonfer, M.; Cohen, H.; Sloan, J.; Hutchison, J. L.; Tenne, R. *Wear* **1999**, *229*, 975.
(24) Homyonfer, M.; Alperson, B.; Rosenberg, Y.; Sapir, L.; Cohen, S. R.; Hodes, G.; Tenne, R. *J. Am. Chem. Soc.* **1997**, *119*, 2693.
(25) Remskar, M.; Skraba, Z.; Ballif, C.; Sanjines, R.; Levy, F. *Surf. Sci.* **1999**, *433−435*, 637.
(26) Rothschild, A.; Frey, G. L.; Homyonfer, M.; Tenne, R.; Rappapport, M. *Mater. Res. Innov.* **1999**, *3*, 145.
(27) Margulis, L.; Tenne, R.; Iijima, S. *Microsc. Microanal. Microstruct.* **1996**, *7*, 87.
(28) Mastai, Y.; Homyonfer, M.; Gedanken, A.; Hodes, G. *Adv. Mater.* **1999**, *11*, 1010.
(29) Zhu, Y. Q.; Hu, W. B.; Hsu, W. K.; Terrones, M.; Grobert, N.; Hare, J. P.; Kroto, H. W.; Walton, D. R. M.; Terrones, H. *Chem. Phys. Lett.* **1999**, *309*, 327.
(30) Feldman, Y.; Wasserman, E.; Srolovitz, D. J.; Tenne, R. *Science* **1995**, *267*, 222.
(31) Srolovitz, D. J.; Safran, S. A.; Homyonfer, M.; Tenne, R. *Phys. Rev. Lett.* **1995**, *74*, 1778.
(32) Feldman, Y.; Frey. G. L.; Homyonfer, M.; Lyakhovitskaya, V.; Margulis, L.; Cohen, H.; Hodes, G.; Hutchison, J. L.; Tenne, R. *J. Am. Chem. Soc.* **1996**, *118*, 5362.

10.1021/cm991189k CCC: $19.00 
Published on Web 04/29/2000

Furthermore, turbulence, which appeared to be an important factor previously, is unnecessary for nanotube formation in the new approach. The nanotubes are large and therefore may exhibit improved semiconductor properties: vide infra.[33]

The apparatus employed[29,34] consisted of a water-cooled stainless steel chamber (45 cm i.d.), connected to Ar and $H_2S$ gas sources and to a vacuum pump. Two stainless steel electrode holders, located at the center of the chamber, provided support for a W foil (50 × 5 × 0.025 mm) heater. A $SiO_2$ plate (Goodfellow, 10 × 5 × 1 mm) was placed on top of the heater. After evacuating the chamber, Ar (100 Torr) was introduced, and ∼35 A dc were applied to the heater. Upon attaining ∼1200 °C (optical pyrometry), the chamber was maintained at this temperature for 30 min (stage one). It was then quickly filled with $H_2S$ gas (∼200 Torr), and the current was reduced to ∼30 A, so that the temperature dropped to ∼1000 °C. It was held at this level for 30 min (stage two) and the current was then switched off. During the first stage, we observed the presence of treelike structures on the edges of the $SiO_2$ plate, which were replaced by gray needles by the end of stage two.

The needles were collected and analyzed directly by XRD and SEM. Samples were dispersed ultrasonically in acetone and, after 5 min, were transferred for TEM measurement to a Cu grid coated with a holey carbon film. The XRD examination was carried out on Siemens D-5000 equipment (Cu Kα radiation), with a 0.02 deg/min scanning rate (operating at 40 mA/40 kV). The following equipment was used as appropriate: SEM (Leo 5420, 10−20 keV), TEM (H-7100, 120 keV; CM200, 200 keV; JEM-4000, 400 keV); energy-dispersive X-ray (EDX) using a Noran Instruments detector attached to a CM-200, element ≥ B.

The product (Figure 1a) consists of randomly distributed long and fairly uniform diameter $WS_2$ nanotubes (up to several tens of micrometers long, ∼10−100 nm diameter), accompanied by only a small quantity of nanoparticles. Careful examination showed that most of the tubes exhibited polygonal, rather than circular cross sections. The structural features resembled the $WO_x$ nanorods ($x = 2-3$) reported previously by us (Figure 1b).[29] Figure 1c shows the overall features of the $WS_2$ IF nanotubes under low magnification. Some of the tubes are filled with $WO_x$. Figure 1d illustrates a typical straight hollow-core nanotube (≥30 $\mu$m long with one end embedded in the $WS_2$ matrix). The outcome is a significantly higher proportion of nanotubes relative to nanoparticles. Furthermore, the tubes are of high quality in that they are very straight and relatively long.

The XRD results show (Figure 2) the general phase components of the sample, compared to the simulated XRD pattern of single $WS_2$ crystals. The phase was identified as a $WS_2$, $WO_x$ ($x \cong 2.7-3$), W mixture by consulting the PDF database. From a comparison of the main peak intensities [the (002) peak to $WS_2$] in the chart, we conclude that $WS_2$ dominates and is accompanied by a small amount of W and a trace of $WO_x$. Furthermore, it is possible to obtain the average diameter (∼30 nm) based on the Debye−Scherrer formula, together with the approximate number of layers (∼10−20) within nanotubes by carefully examining the (002) peak profile and its half-width.

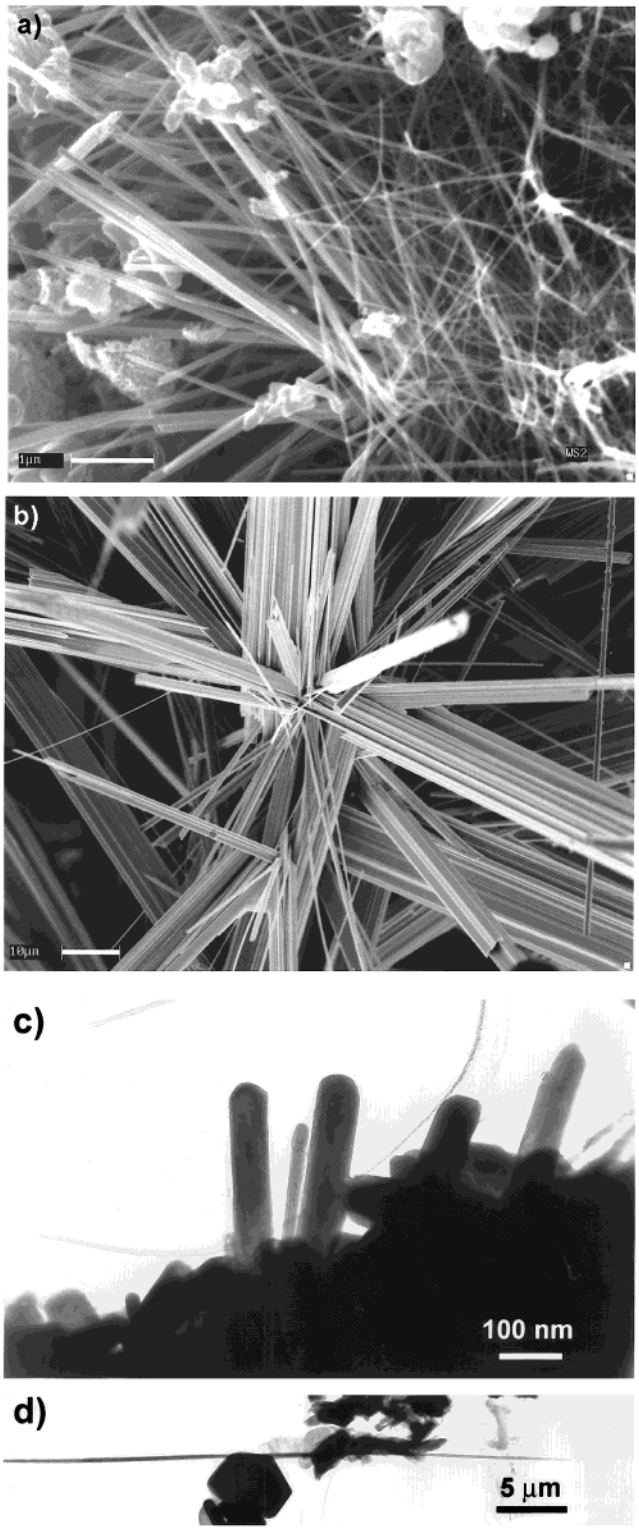


**Figure 1.** (a) Randomly distributed $WS_2$ nanotubes, relatively free of polyhedral particles; (b) $W_{18}O_{49}$ nanorods; (c) nanotube bundles; and (d) a very long nanotube. Parts a and b are SEM images; parts c and d are TEM images.

In our earlier paper,[29] we successfully prepared $WO_x$ nanorods by heating a $SiO_2$ plate with a W heater, probably via

$$W + xSiO_2 \rightarrow WO_x + xSiO \quad (1)$$

(33) Seifert, G.; Terrones, H.; Terrones, M.; Jungnickel, G. Frauenheim, T. Submitted to *Phy. Rev. Lett.*

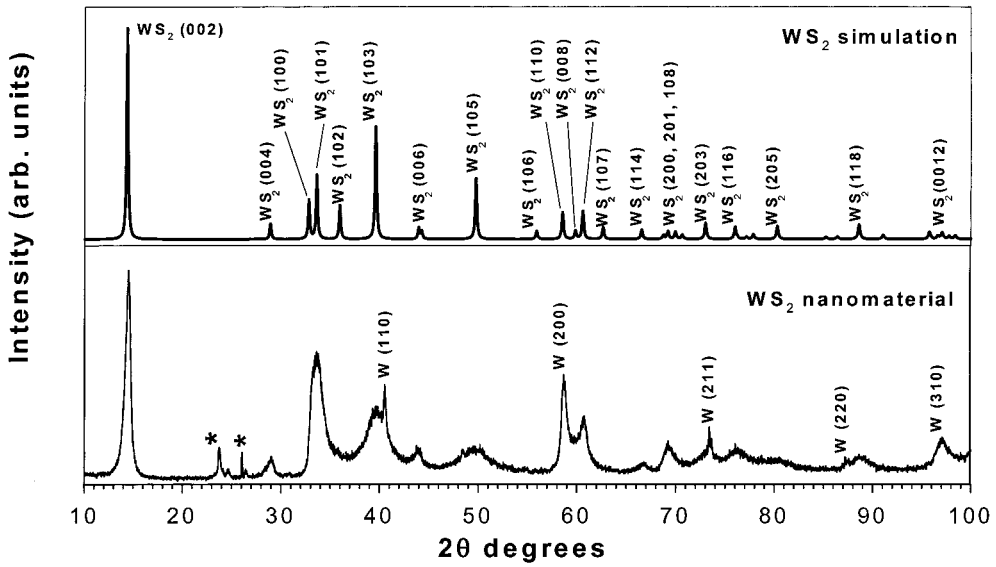


**Figure 2.** XRD profile of $WS_2$ nanotubes: The $WS_2$ phase was indexed in the simulation pattern (upper); the peaks marked (*) correspond to $W_{18}O_{49}$, and W (*hkl*) represents W phase.

According to XRD analysis and HRTEM, we concluded that the resulting nanorods consisted mainly of $W_{18}O_{49}$. Following the procedure developed by Tenne and co-workers,[30−32] we introduced $H_2S$ into our system to generate $WS_2$ IF nanotubes from $WO_x$ nanorods:

$$WO_2 + 2H_2S \rightarrow WS_2 + 2H_2O \qquad (2)$$

The XRD result (Figure 2) supports the conclusion that reaction 2 had occurred as a second stage. $H_2S$ is unlikely to react directly with the W when $WO_x$ is present in the system during stage two ($WO_x$ covering the edges of the W heater). Given the experimental conditions (~1000 °C), we surmise that $H_2S$ may also decompose on the hot W surface, generating S and $H_2$.

Evidence for this conjecture is based upon the fact that at the end of the experiment, a pasty S deposit was found at the top of the inner (water-cooled) wall. This S deposit may contain water generated in reaction 2. However, if $H_2S$ reaches the $WO_x$ surface, held at a relatively low temperature, $WS_2$ is presumably formed more quickly than $H_2S$ decomposes.

An important feature of the present method lies in the omission of directly administered $H_2$, which was a key component in the original IF nanotube production method.[32] As noted above, $H_2$ may well be generated from $H_2S$, but the amount appears to be minimal when compared with the 5% concentration, introduced directly by Feldman et al.[32] In the present method of producing $WS_2$ in the absence of directly administered $H_2$, $WS_2$ nanotubes appear to form by direct reaction of $WO_x$ with $H_2S$. During each stage of our experiment, the gas pressure was kept constant, except for a brief period when $H_2S$ gas was introduced into the chamber. Thus, turbulence was minimized and does not appear to be important for IF nanotube growth in this method.

We believe that reactions 1 and 2 are primarily responsible for generating IF nanostructures (including polyhedral particles). One advantage of the method described in this paper lies in the continuous in-situ production of $WS_2$. The success of the technique is possibly because $W_{18}O_{49}$ is formed directly from W and $SiO_2$, rather than via $WO_3$. Thus, fracture of $WO_3$ during the production is avoided. Furthermore, by not moving the $WO_x$ nanorods at the onset of stage two, we have minimized the damage to them, leading to large nanotubes rather than polyhedral particles. This outcome is important because a recent calculation[33] has revealed that, like their bulk crystals, $WS_2$ nanotubes should behave as semiconductors. However, larger diameter tubes have large band gaps, whereas smaller nanotubes have small band gaps.

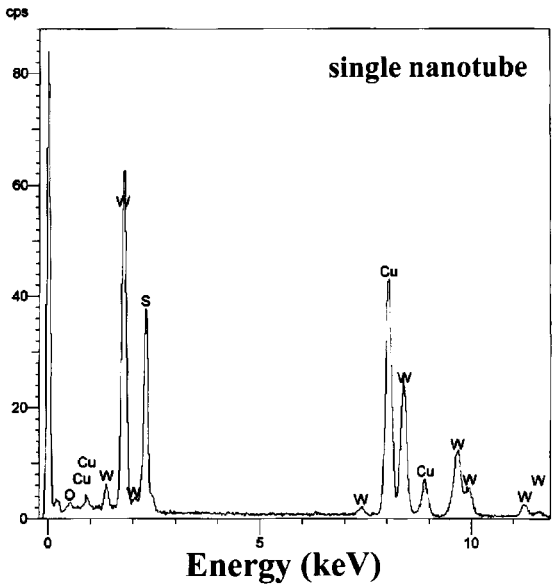


**Figure 3.** EDX of a single $WS_2$ nanotube. The Cu peaks arise from the Cu grid used for TEM examination.

EDX measurements were used to characterize the overall chemical composition of the product, in particular that of a single tube. The results (Figure 3) also prove that $WS_2$ is the dominant phase; only a tiny peak indicates the presence of O, which corresponds to the occurrence of the $WO_x$ phase. In this case, HRTEM measurements indicate that the tubes are fully, or partly filled with elongated single crystals. The encapsulated phases usually exhibit a crystalline fringe, ~0.38 nm, which matches the crystalline lattice of $WO_x$ nanorods. This result agrees well with a comprehensive

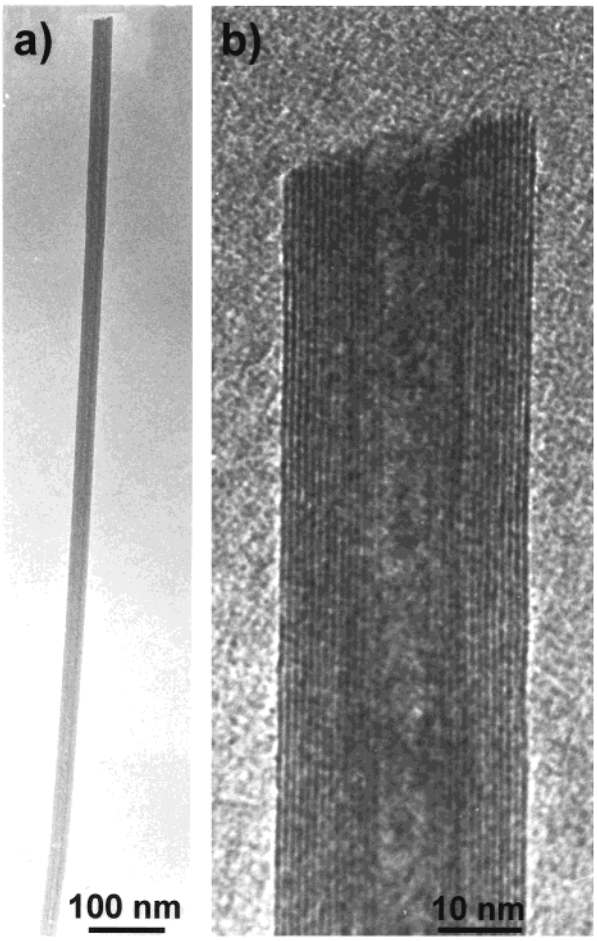


**Figure 4.** HRTEM images: (a) a typical nanotube and (b) tube tip enlargement.

study by Sloan et al.[35] who, using HRTEM, characterized both defect and ordered $WO_x$ ($x = 2-3$) crystals encapsulated by the $WS_2$ nanostructures. Note that the present procedure is continuous and therefore, during the second stage, reaction 1 may continue, resulting in $WO_x$ (indicated by the two peaks in Figure 2). This should lead to the longer $WS_2$ tubes arising from part conversion of $WO_x$ nanotubes.

These in-situ-generated $WS_2$ IF nanotubes exhibit crystalline features differing from those of carbon nanotubes. Some of the IF nanotubes appear to be dislocated. In general, we observe $WS_2$ nanotubes with fully open tips (Figure 4), in contrast with carbon nanotubes which are nearly always closed. For carbon nanotubes, dangling bonds appear able to automatically "seal" the open tips when the growth is terminated.[36] However, it seems that for $WS_2$, no such sealing process occurs. This open-tipped feature means that IF nanotubes exhibit a morphological similarity to the ceramic nanotubes (vanadium oxide), which are thought to grow according to a roll-up model.[17−18]

Figure 5a shows the presence of layer dislocations in the walls (arrowed), which appear to occur at the outer, rather than the inner layers, probably because the outer

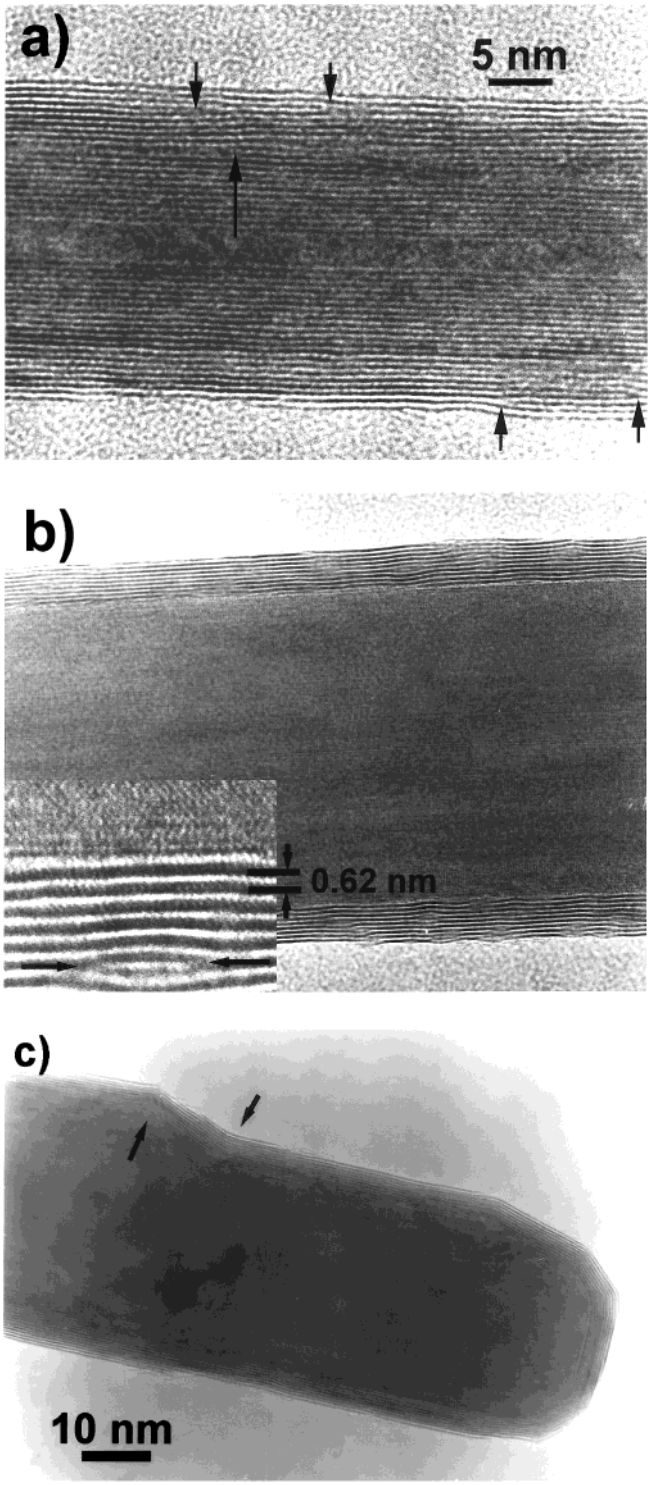


**Figure 5.** HRTEM images: (a) layer dislocation (arrowed) occurring at the outer shells and (b) high-density layer defects within the tube walls (the insert is an enlargement of the defect (arrows), and the defect-free layers are separated by ~0.62 nm); and (c) nanotube with different diameter (arrowed).

shells are subject to less strain than are the inner shells. In some cases, we observed defective structures between the tube walls (Figure 5b). Under TEM projection, it is not difficult to visualize the inserted tiny atomic planes (arrows), although we are not clear as to the actual outer curvature of the tube. Because of the high density and asymmetric distribution of these defects, it seems that they may not occur around the entire tube body but are confined to small regions. Indeed, they appear to be a

(34) Zhu, Y. Q.; Hsu, W. K.; Terrones, M.; Grobert, N.; Hare, J. P.; Terrones, H.; Kroto, H. W.; Walton, D. R. M. *J. Mater. Chem.* **1998**, *8*, 1859.

(35) Sloan, J.; Hutchison, J. H.; Tenne, R.; Feldman, Y.; Tsirlina, T.; Homyonfer, M. *J. Solid State Chem.* **1999**, *144*, 100.

bifurcation point of two layers. For this nanotube, this type of defect is often present, suggesting that layer defects tend to occur in the $WS_2$ system. Since crystallographic shear structural defects often occur in encapsulated $WO_x$ phases, and in the conversion process from $WO_x$ nanorods to $WS_2$ nanotubes, it is possible that these bifurcation points originate from defects in the $WO_x$ shear planes. The HRTEM measurement by Sloan et al. clearly reveals how encapsulated $WO_x$ defects influence the $WS_2$ outer curve structure.[35] The cause of this type of defect and the effect on nanotube mechanical and electronic properties warrants further investigation.

The SEM result shows that the nanotubes exhibit polygonal cross sections. TEM measurements reveal the presence of numerous uneven interlayer distances, in some cases $\geq$0.62 nm on either side of the tubes, which may confirm this fact.[37] Such polygonal features characterized our previous $WO_x$ nanorod sample. Furthermore, we have verified, by SEM, that some of the nanorods possess a square cross-section. Because of the intrinsic crystalline nature of $WO_x$, the two neighboring basal planes within a nanorod are usually located at $\sim$90° to each other. Therefore, a question may arise concerning the atomic network arrangement in constructing a $WS_2$ nanotube. We think that the established $WO_x-WS_2$ conversion mechanism for IF nanotube growth[31] can generally be applied to our process. The nanotube or nanoparticle growth has been thought to originate from the existing $WO_x$ nanorod or nanoparticle by an oxide replacement process. Previous HRTEM observations provide experimental support for this conjecture.[32] Significant volume or shape changes do not appear to occur during nanotube growth through a gas−solid-phase reaction ($H_2S-WO_x$ reaction). Therefore, the initial features of these $WO_x$ nanorods might be inherent in the nanotubes, which is why our nanotubes are longer (and contain less IF polyhedral particles) than those converted from $WO_x$ powder. More than half of the $WO_x$ nanorods exhibit polygonal cross sections, thus the IF nanotubes will retain their shape, as suggested by Sloan et al.[35] However, the five- or seven-membered ring configurations for carbon nanotubes forming a facet,[38] may also occur here (Figure 5c). For IF nanotubes, three- or four-membered rings can also cause a positive curvature in the $WS_2$ crystal lattice.[35] It is difficult to provide a coherent $\sim$90° connections in most cases. This polygonal cross-sectional feature might be the main cause of the high-density defects within the tube walls.

In the studies by Feldman et al.,[30−32] the XRD measurements on the (002) peak of the IF materials indicated that the $d$ ($= c/2$) spacing increased by $\sim$2%, which is evidence for strain relief. In our XRD studies, the same $d_{002}$ enlargement was also apparent. By comparison with simulated diffraction patterns for $WS_2$ single crystals, we noticed that the intensity of the (002) peak arising from the successive closely spaced layers, tends to be quite sharp. However, the higher angle peaks, e.g. (004), (006), (008), and (0012), arising from the long period layers of the crystal are obviously broadened. This indicates a poorer long distance layer order within a nanotube, a result consistent with HRTEM observations. The asymmetrically broadened (100) and (101) peaks, determined by the 3-D atomic positions within the IF nanotubes, might be caused by network rotation along the tube axis ($\langle 100 \rangle$ direction), analogous to helical carbon nanotube structures. Unfortunately, we cannot determine the actual helix angles between different layers. It is noteworthy that the (004) peak intensity for the IF nanotubes may be influenced by overlap with complex $WO_x$ phases present in the sample. The EDX results revealed the presence of a small amount of O. The HRTEM analysis confirmed that some $WO_x$ crystals are encapsulated in $WS_2$ tubes. Thus, $WO_x$ phases must contribute to the XRD intensities for some peaks. In contrast with our previous XRD study on $WO_x$ nanorods, we can only identify the two obvious peaks, and we suggest that they also correspond to the $W_{18}O_{49}$ phase. The other peaks are too weak to be indexed. This analysis also supports Feldman et al.'s conjecture that IF nanotube growth starts with the reduced $WO_x$ phase, particularly $W_{18}O_{49}$.[32] It is noteworthy that, because of the numerous intermediate phases for $WO_x$, it is always difficult, from XRD measurements, to identify one particular encapsulated $WO_x$ phase precisely in a nanotube. HRTEM and ED methods can provide a better understanding of the $WO_x$ encapsulated phases.[35]

In conclusion, we have successfully generated relatively long IF $WS_2$ nanotubes, in good yield and high purity using a simplified in-situ process. The nanotubes are formed directly from $WO_x$ nanorods created from W and $SiO_2$ during the first stage. Structural similarities and differences between IF and carbon nanotubes have been probed, and it is a particularly noteworthy feature of these $WS_2$ tubes that some their tips are fully open.

**Acknowledgment.** We thank the Royal Society (Y.Q.Z., W.K.H., B.H.C.), the JFCC (Y.Q.Z., N.G.), Conacyt-México and DGAPA-UNAM IN 107-296 (H.T.), EPSRC (W.K.H.), and Max-Planck Society Fellowship (B.Q.W.) for financial support. We are grateful to J. Thorpe and D. Randall (Sussex) for assistance with TEM and SEM facilities.

CM991189K

(36) Iijima, S. *Mater. Res. Bull.* **1994**, *19*, 51.
(37) Liu, M.; Cowley, J. M. *Ultramicroscopy* **1994**, *53*, 333.
(38) Iijima, S.; Ichihashi, T. *Nature* **1993**, *361*, 603.